Journal of Geospatial Science and Technology
Vol. 02 No. 02 2024
https://journal.ugm.ac.id/v3/jgst

Effect of Tropospheric Correction on Long Term Sentinel-1 SAR Measurement: Application to the Surface Displacement Observation along Opak Fault, Yogyakarta

Insan Mafaazan[1], Hidayat Panuntun[2]
[1]Teknologi Survei dan Pemetaan Dasar, Departemen Teknologi Kebumian, Sekolah Vokasi, Universitas Gadjah Mada, Indonesia
[2]Lab. Geomatika, Departemen Teknologi Kebumian, Sekolah Vokasi, Universitas Gadjah Mada, Indonesia

Research Article
DOI:
10.22146/jgst.v2i2.17064

correspondence:
insanmafaazan@mail.ugm.ac.id

Article history:

Received:
17-10-2024
Accepted:
31-12-2024
Published:
31-12-2024

ABSTRACT

Sentinel-1 is a remote sensing satellite launched by the European Space Agency (ESA). It is equipped with a radar system that can take measurements over a wide area with high accuracy (cm-mm) and long-term observations. However, one of the main factors affecting long-term SAR measurements' accuracy is the presence of tropospheric layers within the atmosphere. To determine how much influence this tropospheric effect has, two processing scenarios are performed, namely with and without tropospheric correction, respectively. LiCSBAS is used to perform processing with the time series analysis method. This project uses interferogram data from the Sentinel-1 SAR image with temporal ranging from 2015 to 2023. The research location is in Yogyakarta. Noise due to the presence of tropospheric layer was modeled and removed using Generic Atmospheric Correction Online Service (GACOS). The results show that tropospheric correction can improve the results by reducing the standard deviation in the interferogram phase up to 40%. Based on the results, without tropospheric correction, the maximum vertical displacement is 32.64 mm. With tropospheric correction, the maximum vertical displacement is 34.58 mm. The result suggests that noise from the tropospheric layer might underestimate the vertical displacement. Hence, applying the correction, especially for long-term InSAR measurement, is important.

Key words: InSAR, unwrapped interferogram, GACOS, LiCSBAS, time series analysis, vertical displacement

1. Introduction

Sentinel-1 is a remote sensing satellite launched by the European Space Agency (ESA) as part of the Copernicus program (Attema et al., 2009). Remote measurements using the Sentinel-1 satellite equipped with Synthetic Aperture Radar (SAR) have become one of the main tools in earth monitoring, allowing for wide-coverage, high-accuracy and continuous mapping of earth surface deformation (Xue et al., 2020). However, to obtain high accuracy and precision in long-term measurements such as monitoring ground displacement or geological surface changes that occur over several years, there are factors that need to be taken into account, namely the influence of the troposphere (Zhou et al., 2009).

The troposphere is the lowermost layer of the atmosphere closest to the Earth's surface. This layer is characterized by rapid fluctuations in air temperature, pressure, and humidity. Tropospheric effects in SAR measurements can lead to incorrect phase displacement in the radar image, which in turn can result in inaccuracies in distance measurements and surface deformation (Yu et al., 2018b).

It is important to understand how tropospheric effects can affect the long-term measurement results of Sentinel-1 and how tropospheric correction can be applied to address these issues. Tropospheric correction is a process that involves accounting for and compensating for atmospheric effects in SAR measurements. This is necessary to ensure that long-term data from Sentinel-1 is reliable, accurate and useful in understanding and monitoring changes on the Earth's surface. One pivotal study by Panuntun et al. emphasizes the importance of tropospheric correction in InSAR measurements, particularly in the context of the 2018 Palu earthquake. Their findings demonstrate that applying GACOS significantly improved the accuracy of line-of-sight (LOS) displacement measurements when compared to uncorrected data, thereby validating the necessity of such corrections in post-seismic analysis (Panuntun et al., 2022). The effectiveness of various tropospheric correction models has been further explored by Yu et al. (2024), who assessed different models in the context of ground

deformation monitoring in Zhejiang Province, China. Their study indicates that tailored correction models can substantially reduce atmospheric noise, thereby improving the reliability of InSAR data. Additionally, Watson et al. (2022) corroborate this by noting that atmospheric noise is often the largest source of error in InSAR data, and they successfully utilized GACOS to mitigate these errors in their observations across southwestern Iran. Moreover, Kirui et al. (2021) highlight the significance of numerical weather products in tropospheric corrections, demonstrating that neglecting tropospheric noise can lead to misinterpretations of deformation signals. Their review of various correction techniques illustrates the evolving landscape of tropospheric correction methodologies and their integration into InSAR applications. The study by Zhang et al. (2022) also contributes to this discourse by proposing an adaptive fusion method that combines multiple sources of tropospheric delay estimates, thereby enhancing the accuracy of deformation measurements.

The necessity for tropospheric corrections in InSAR observations along the Opak Fault in Yogyakarta is underscored by the significant atmospheric effects that can distort the measurements of ground deformation. The Opak Fault is a tectonically active region, and accurate monitoring of its behavior is crucial for understanding seismic risks and potential hazards in the area. The troposphere introduces phase delays in radar signals, which can lead to misinterpretations of ground movement if not properly corrected. One of the primary reasons for implementing tropospheric corrections is the inherent variability of atmospheric conditions, which can introduce significant noise into InSAR data. Atmospheric contamination can severely affect the accuracy of InSAR measurements, particularly in regions with complex terrain like Yogyakarta, where the elevation-dependent tropospheric signals can vary widely (Yu et al., 2018a). This variability can lead to errors in the estimation of ground deformation, as the atmospheric delays can be on the order of several centimeters, potentially masking or mimicking actual tectonic movements (Yu et al., 2018b). In this paper, we will further discuss the influence of the troposphere on Sentinel-1 long-term measurements, the tropospheric correction methods used, and the importance of applying these tropospheric corrections in long-term monitoring applications. By understanding the importance of using tropospheric corrections to improve the accuracy of Sentinel-1 data, we can harness the great potential of the Sentinel-1 satellite for better environmental monitoring.

Figure 1. Map of the study area.

2. Data

The study area is located in the city of Yogyakarta and its surroundings. The study area has geographical boundaries with coordinates 110° 8' 51" - 110° 39' 13" E and 8° 6' 0" - 7° 43' 12" S. Within the study area there is also the Opak Fault that runs along the Opak River itself. The map of the research study area is shown in Figure 1. In this study, Sentinel-1 SAR image interferogram data was used with the observation period from January 2015 to January 2023. This interferogram data comes from Copernicus Sentinel data that has been modified and analyzed by the Centre for the Observation and Modelling of Earthquakes, Volcanoes and Tectonics (COMET) (Lazecký et al., 2020). The number of sample points consisted of 5 points spread across the research study area and were considered representative of the surrounding data. The sample points were selected based on the locations of GNSS observation points identified by Widjajanti et al. (2020). This selection aims to enable comparisons for validating the observation results obtained through InSAR analysis. The software used consists of Ubuntu 22.04, LiCSBAS (Morishita et al., 2020), Generic Mapping Tools (GMT) (Wessel et al., 2019), Visual Studio Code, Microsoft Word and Microsoft Excel. The specifications of the Sentinel-1 image interferogram data used in this study are shown in Table 1.

Table 1. Sentinel-1A image interferogram data specification

No	Description	Orbit Direction	
		Ascending	Descending
1	Frame ID	127A_09749_121312	076D_09725_121107
2	Acquisition Date	January 30, 2015 - January 12, 2023	January 26, 2015 - January 08, 2023
3	Products	1395 interferograms	687 interferograms
4	Epochs Processed	100%	100%
5	GACOS	100%	100%
6	Recording Mode	IW	IW
7	Polarization	VV+VH	VV+VH
1	Frame ID	127A_09749_121312	076D_09725_121107

3. METHOD

3.1. Preprocessing

The initial stage carried out in this study is the preparation of unwrapped interferogram data and tropospheric correction data (GACOS) that will be used in the entire processing step. The data download process is semi-automatic with the LiCSBAS python package integrated with the data provider server. Data collection is done by determining the frame id number with the image covering the research study area. The settings that need to be applied to LiCSBAS to download data are inputting the start and end dates and the frame id number for defining the image frame. This study uses two frames of Sentinel-1 image interferogram data consisting of interferogram data with ascending and descending orbit directions.

3.2. Interferograms Data Accuracy Test

The interferogram data was processed with two scenarios, namely using and without using tropospheric correction (GACOS). In general, the two multi-interferogram processing scenarios have the same flow chart such as clipping, masking, data quality checking, Small Baseline Network Inversion process, standard deviation estimation, to masking and filtering time series data.

Basically, interferograms still have phase noise caused by signal delays during measurement. Factors that can interfere with the signal during recording are water vapor, temperature, and tropospheric pressure that vary in various conditions. Measurement errors caused by these tropospheric influences can reach 10 cm or more (Bekaert et al., 2015). Removal of tropospheric influences before spatiotemporal filtering using independent data can improve the accuracy of displacement time series. GACOS data provides high-resolution tropospheric delay maps in near real time, so it can be used to correct tropospheric noise in interferograms (Yu et al., 2018b). LiCSBAS will automatically calculate the standard deviation of the interferogram data before and after GACOS correction, along with the reduction level of each interferogram data. The interferograms before and after correction will be recreated to help check the effect of the GACOS correction itself. In addition, interferograms that have failed recording frames and have incomplete data will have a negative impact on processing. Therefore, poor quality data will be identified and corrected based on statistics including the average coherence and percentage of valid pixel values in the interferogram.

Interferogram correction is done with several approaches, namely by utilizing the redundancy of the interferogram network and closing the phase loop (Xiao et al., 2021). Interferograms that have many wrapping errors will be automatically removed because the correction process is done on an image-by-image basis, not on a pixel-by-pixel basis (Yunjun et al., 2019). For example, if there are three images ($\varphi 1$, $\varphi 2$, and $\varphi 3$) and three unwrapped interferograms ($\varphi 12$, $\varphi 23$, and $\varphi 13$), their loop phases are calculated by equation 1 (Biggs et al., 2007).

$$\Phi 123 = \varphi 12 + \varphi 23 - \varphi 13 \quad (1)$$

If there are no errors in the three interferograms, then the loop phase value should be close to zero. However, if there are interferograms containing wrapping errors, then the loop phase value will approach a multiple of 2π. The Root Mean Square (RMS) value indicates how many pixels with packing errors are included in the loop phase.

3.3. Time-Series Processing

The estimated velocity value at a pixel is obtained based on a series of displacement data in the interferogram network formed. For example, by considering the interferogram or displacement between two acquisitions that have had their incremental displacement values summed sequentially (Schmidt and Bürgmann, 2003). The cumulative displacement for each acquisition is calculated by summing the incremental displacements. The average displacement velocity is then obtained from the cumulative displacement by the least-square's method. The estimated velocity standard deviation value of the cumulative displacements was obtained using the percentile bootstrap method (Xu, 2009). The bootstrap method creates a data set by taking randomly with replacement data. The velocity value and its standard deviation will be calculated at each iteration. A high standard

deviation estimate indicates that the time series displacement value is not linear. Spatiotemporal filters can also be used to separate the noise component from the displacement time series (Hooper et al., 2012).

3.4. Decomposing Line of Sight (LOS)

The time series results in the form of Line of Sight (LOS) displacements will be decomposed to obtain 2.5D displacement values, namely in the direction of vertical (Uplift-Downlift) and horizontal (East-West) displacements. Decomposing LOS can be done with a minimum of two independent measurements that include ascending and descending orbit directions. Decomposing LOS can be applied with equation 2 below (Fuhrmann and Garthwaite, 2019).

$$\begin{pmatrix} V_{los}^{a} \\ V_{los}^{d} \end{pmatrix} = \begin{pmatrix} cos\theta^{a} & -cos\alpha^{a} sin\theta^{a} \\ cos\theta^{d} & -cos\alpha^{d} sin\theta^{d} \end{pmatrix} \begin{pmatrix} V_{v} \\ V_{e} \end{pmatrix} \quad (2)$$

Where the scripts (a) and (d) above indicate the ascending and descending orbit directions, α is the azimuth of the LOS vector, θ is the incidence angle, Vv and Ve are the horizontal (east-west) and vertical velocities. In the equation, the LOS velocities used in the ascending and descending orbit directions have the same time period and the same spatial resolution. The LOS displacement rate will be geocoded and interpolated into the same geographic grid to estimate the east-west and vertical displacement rates.

4. RESULT AND DISCUSSION

4.1. Line of Sight (LOS) Displacement Results

The value of land surface displacement in Yogyakarta City and its surroundings was successfully obtained using the time series analysis method. The application of tropospheric correction to the interferogram data shows that the standard deviation values before and after using the correction have a linear distribution. This means that each scatter plot after correction has the same value as before correction and is located on the matching line, so the interferogram model that has been corrected with GACOS data has good accuracy. The results show that tropospheric correction of the interferograms used in this area study can reduce the standard deviation of the interferogram phase by 40%. The degree of reduction of the tropospheric influence on the interferogram depends on the tropospheric conditions at the time of the Sentinel-1 SAR data acquisition. Therefore, the availability of GACOS data in accordance with the temporal interferogram data needs to be ensured before making deformation observations using Sentinel-1 data. Results related to standard deviation information before and after the application of tropospheric correction using GACOS data can be seen in Figure 2.

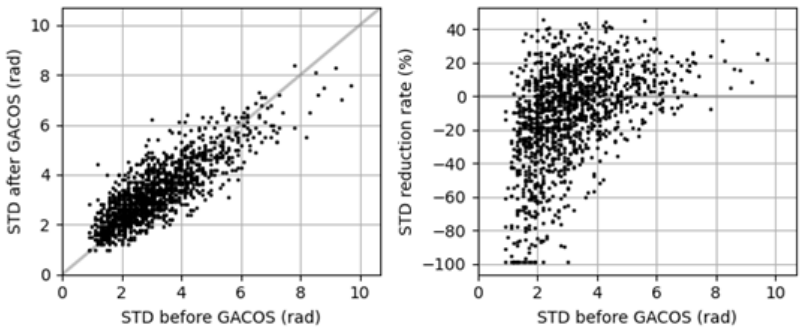

Figure 2. Scatter plot of standard deviation before and after GACOS correction.

In addition, the LOS displacement value on January 12, 2023 has been successfully obtained with the reference date of January 30, 2015. Figure 3, shows the cumulative map of LOS displacement for ~8 years from 2015 to 2023. Visually, a pattern of land surface uplift is found around the areas of sample points TGD0, TGD1 and SG5E. In contrast, the area around the location of points OPK6 and OPK4 experienced a pattern of land subsidence. When viewed from the processing results with and without tropospheric correction, both have the same movement pattern. This can be seen in more detail in the results of the LOS displacement time series export at each sample point. Based on the time series obtained, it shows that the LOS displacement value without GACOS correction tends to underestimate the observed displacement value. This is evidenced by the cumulative LOS displacement values with tropospheric correction are 42.54 at TGD0, 32.06 mm at TGD1, 4.71 mm at OPK4, -21.68 mm at OPK6 and 19.77 mm at SG5E. Meanwhile, without tropospheric correction, the cumulative displacement values were 42.92 mm at TGD0, 22.88 mm at TGD1, 5.36 mm at OPK4, -17.75 mm at OPK6 and 26.31 mm at SG5E. Therefore, InSAR observations using Sentinel-1 images should be applied tropospheric correction during processing.

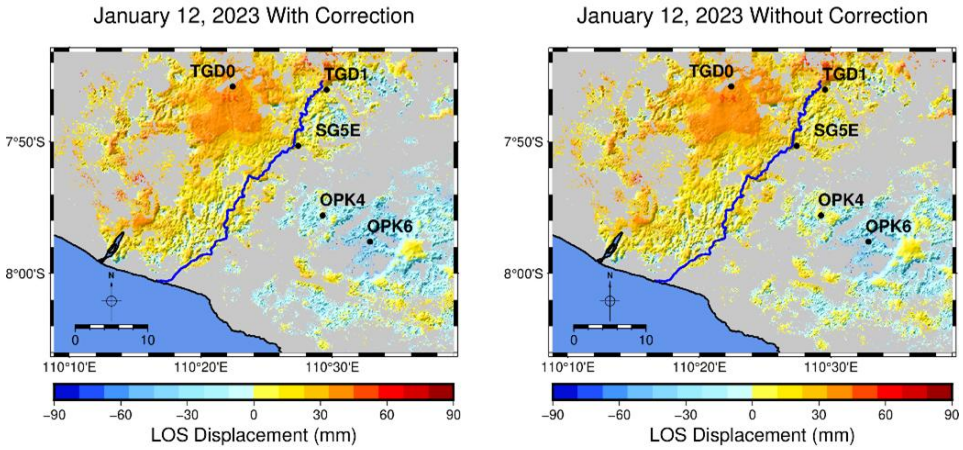

Figure 3. Time windows of LOS displacement in 2023. The blue line represents the location of the Opak River. Black dots represent the location of sampling points.

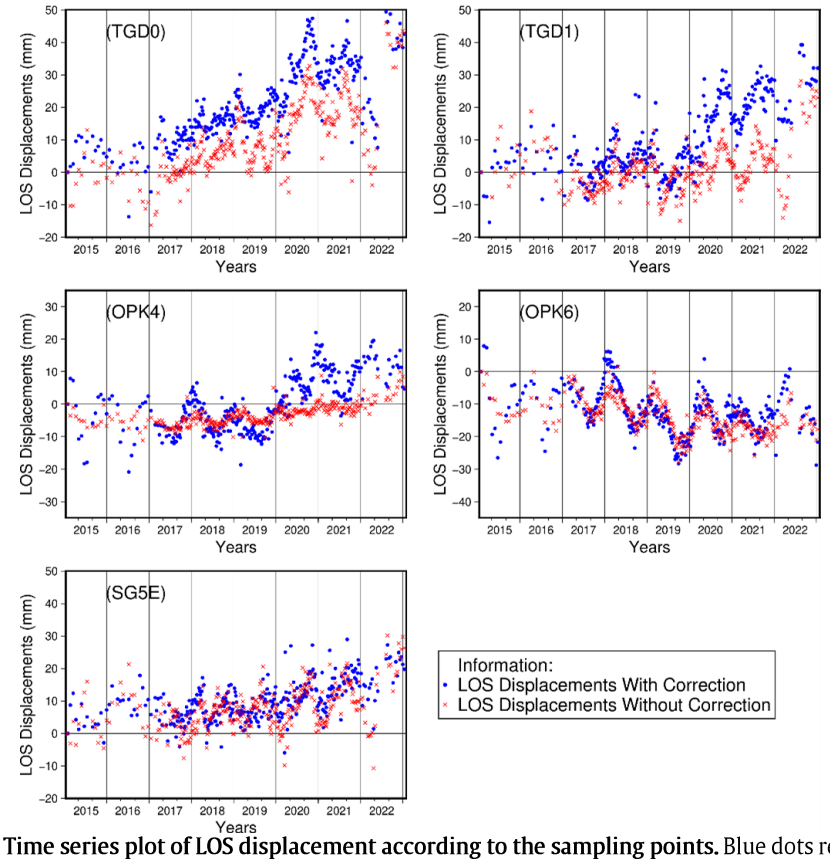

Figure 4. Time series plot of LOS displacement according to the sampling points. Blue dots represent the time series with GACOS correction. The red cross represents the time series without GACOS correction.

4.2. Vertical Displacement Results

Vertical displacement results have also been obtained from the LOS decomposition process. The cumulative vertical displacement values were extracted from two LOS with different orbital directions with reference dates of January 2015 to January 2023. The vertical displacement values also have linear results like the LOS displacement results. The visual display of the cumulative vertical displacement can be seen more clearly in Figure 5. The vertical displacement value also shows that without using tropospheric correction, the value tends to be underestimated than the tropospheric corrected displacement value. The troposphere-corrected vertical displacement has a cumulative value of 34.58 mm at TGD0, 24.63 mm at TGD1, 6.46 mm at OPK4, -21.38 mm at OPK6, and 16.09 mm at SG5E. Meanwhile, the cumulative value of vertical displacement without correction obtained was 32.64 mm at TGD0, 16.29 mm at TGD1, 7.20 mm at OPK4, -19.37 mm at OPK6, and 19.91 mm at SG5E. The vertical displacement time series can be seen more clearly in Figure 6.

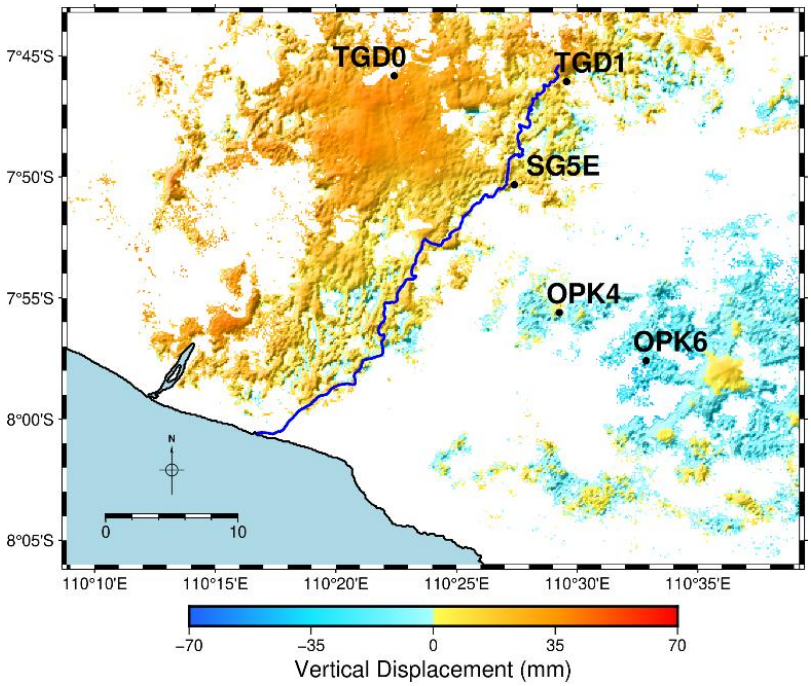

Figure 5. Time windows of vertical displacement in 2023 with reference in 2015. The blue line represents the location of the Opak River. Black dots represent the location of sampling points.

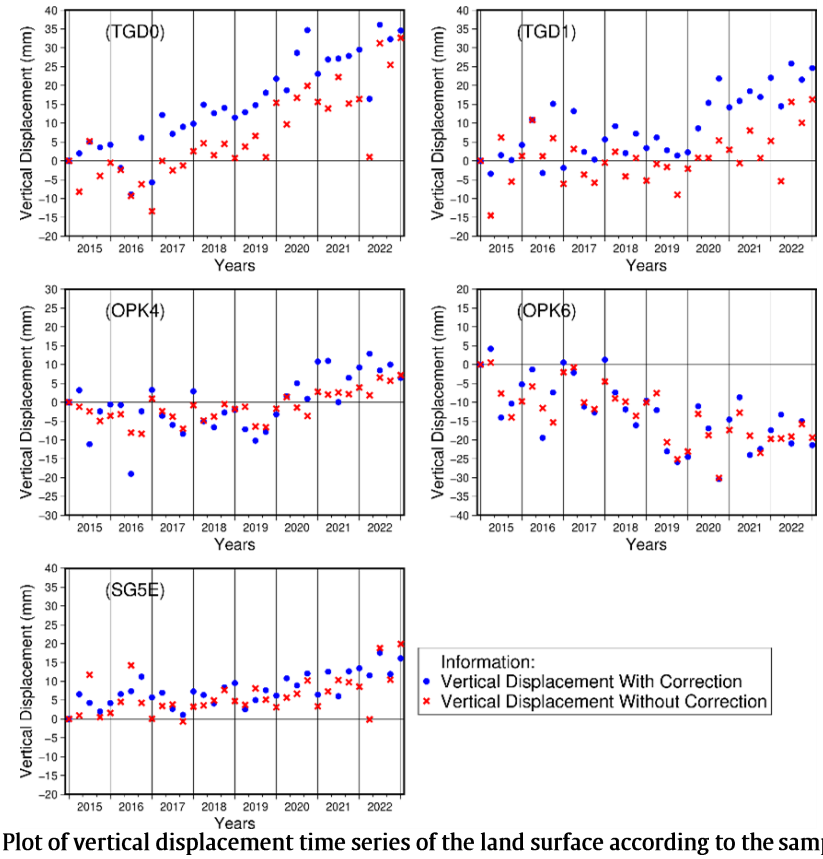

Figure 6. Plot of vertical displacement time series of the land surface according to the sampling points. Blue dots represent the time series with GACOS correction. The red cross represents the time series without GACOS correctionwithout GACOS correction.

Figure 6 shows a comparison of the estimated values between correction and no tropospheric correction taken at the sample points. The estimated value of vertical displacement without correction experiences a signal delay from the influence of the troposphere which results in an underestimate of the vertical displacement value of the land surface. Based on the vertical displacement values obtained for ~8 years since 2015, vertical displacement has been found in the

western part of the Opak Fault with a maximum displacement value of 34.58 mm. Meanwhile, in the eastern part of the Opak Fault, it was found that the dominant land surface has decreased with a maximum value of -21.38 mm. This vertical movement pattern has also been observed with GNSS (Widjajanti et al., 2020) and has the same movement trend as the observation using Sentinel-1 data (Figure 7). Based on the observation of Sentinel-1 interferogram with tropospheric correction has a value that is consistent with GNSS observations, it can be concluded that the estimated value of the resulting displacement is appropriate.

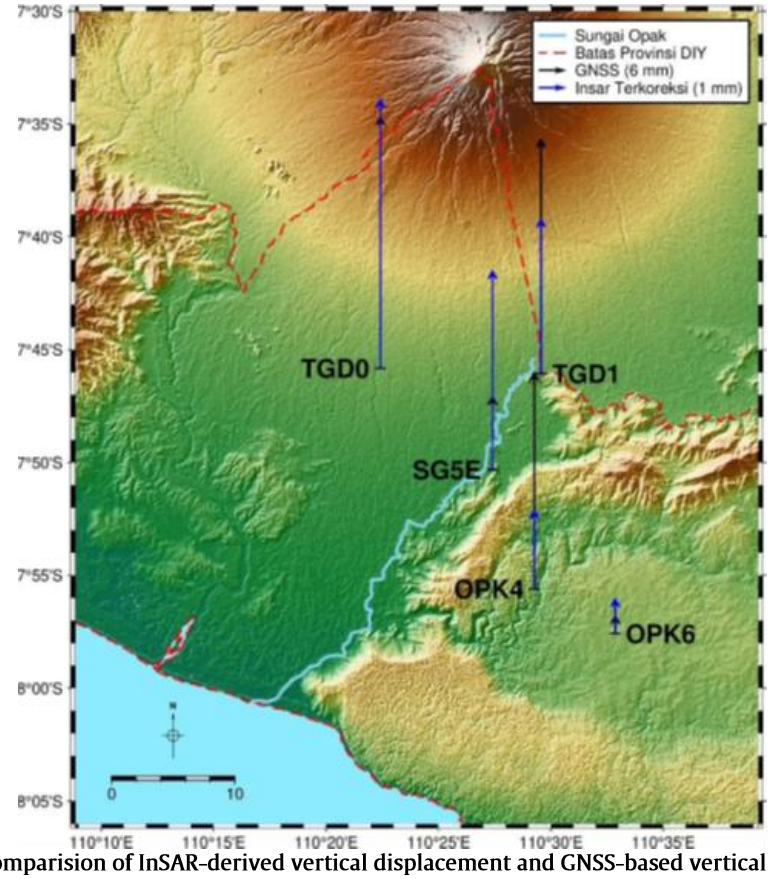

Figure 7. Comparision of InSAR-derived vertical displacement and GNSS-based vertical displacement.

5. CONCLUSION

This study demonstrates the critical role of tropospheric correction in enhancing the accuracy of long-term Sentinel-1 SAR data for monitoring surface displacement along the Opak Fault in Yogyakarta. The application of GACOS data successfully reduced interferogram phase noise by up to 40%, resulting in more reliable deformation measurements. Corrected vertical displacement values, validated against GNSS observations, showed better alignment compared to uncorrected values, which tended to underestimate displacement. These findings emphasize the importance of applying tropospheric corrections to minimize atmospheric effects and ensure the dependability of Sentinel-1 SAR data for geospatial monitoring and tectonic studies. Future research should focus on expanding spatial coverage to other fault zones, developing advanced atmospheric correction models, integrating SAR data with denser GNSS networks, and employing machine learning techniques to enhance temporal analysis and detect anomalies. Additionally, further work could explore 3D deformation modeling for better representation of fault dynamics, assess the impact of seasonal and climatic variations on tropospheric delays, and establish automated monitoring systems to support disaster mitigation and early warning strategies.

6. ACKNOWLEDGMENT

"LiCSAR contains modified Copernicus Sentinel data 2024 analysed by the Centre for the Observation and Modelling of Earthquakes, Volcanoes and Tectonics (COMET). LiCSAR uses JASMIN, the UK's collaborative data analysis environment (http://jasmin.ac.uk)" .

7. REFERENCES

Attema E, Davidson M, Snoeij P, Rommen B, Floury N Sentinel-1 mission overview. In: 2009 IEEE International Geoscience and Remote Sensing Symposium, 12-17 July 2009 2009. pp I-36-I-39. doi:10.1109/IGARSS.2009.5416921

Bekaert DPS, Walters RJ, Wright TJ, Hooper AJ, Parker DJ (2015) Statistical comparison of InSAR tropospheric correction techniques. Remote Sensing of Environment 170:40-47. doi:https://doi.org/10.1016/j.rse.2015.08.035

Biggs J, Wright T, Lu Z, Parsons B (2007) Multi-interferogram method for measuring interseismic deformation: Denali Fault, Alaska. Geophysical Journal International 170 (3):1165-1179. doi:https://doi.org/10.1111/j.1365-246X.2007.03415.x

Fuhrmann T, Garthwaite MC (2019) Resolving Three-Dimensional Surface Motion with InSAR: Constraints from Multi-Geometry Data Fusion. Remote Sensing 11 (3):241. doi:10.3390/rs11030241

Hooper A, Bekaert D, Spaans K, Arıkan M (2012) Recent advances in SAR interferometry time series analysis for measuring crustal deformation. Tectonophysics 514-517:1-13. doi:https://doi.org/10.1016/j.tecto.2011.10.013

Kirui PKe, Reinosch E, Isya N, Riedel B, Gerke M (2021) Mitigation of Atmospheric Artefacts in Multi Temporal InSAR: A Review. PFG – Journal of Photogrammetry, Remote Sensing and Geoinformation Science. doi:10.1007/s41064-021-00138-z

Lazecký M, Spaans K, González PJ, Maghsoudi Y, Morishita Y, Albino F, Elliott J, Greenall N, Hatton E, Hooper A, Juncu D, McDougall A, Walters RJ, Watson CS, Weiss JR, Wright TJ (2020) LiCSAR: An Automatic InSAR Tool for Measuring and Monitoring Tectonic and Volcanic Activity. Remote Sensing 12 (15). doi:10.3390/rs12152430

Morishita Y, Lazecky M, Wright TJ, Weiss JR, Elliott JR, Hooper A (2020) LiCSBAS: An Open-Source InSAR Time Series Analysis Package Integrated with the LiCSAR Automated Sentinel-1 InSAR Processor. Remote Sensing 12 (3):424

Panuntun H, Heliani LS, Suryanto W, Pratama C (2022) Importance of Tropospheric Correction to C-band InSAR Measurements: Application in the 2018 Palu Earthquake. Indonesian Journal of Geography 50 (3):207-213. doi:10.22146/ijg.68984

Schmidt DA, Bürgmann R (2003) Time-dependent land uplift and subsidence in the Santa Clara valley, California, from a large interferometric synthetic aperture radar data set. Journal of Geophysical Research: Solid Earth 108 (B9). doi:https://doi.org/10.1029/2002JB002267

Watson AR, Elliott JR, Walters RJ (2022) Interseismic Strain Accumulation Across the Main Recent Fault, SW Iran, From Sentinel-1 InSAR Observations. Journal of Geophysical Research: Solid Earth 127 (2):e2021JB022674. doi:https://doi.org/10.1029/2021JB022674

Wessel P, Luis JF, Uieda L, Scharroo R, Wobbe F, Smith WHF, Tian D (2019) The Generic Mapping Tools Version 6. Geochemistry, Geophysics, Geosystems 20 (11):5556-5564. doi:10.1029/2019GC008515

Widjajanti N, Pratama C, Parseno, Sunantyo TA, Heliani LS, Ma'ruf B, Atunggal D, Lestari D, Ulinnuha H, Pinasti A, Ummi RF (2020) Present-day crustal deformation revealed active tectonics in Yogyakarta, Indonesia inferred from GPS observations. Geodesy and Geodynamics 11 (2):135-142. doi:https://doi.org/10.1016/j.geog.2020.02.001

Xiao R, Yu C, Li Z, He X (2021) Statistical assessment metrics for InSAR atmospheric correction: Applications to generic atmospheric correction online service for InSAR (GACOS) in Eastern China. International Journal of Applied Earth Observation and Geoinformation 96:102289. doi:https://doi.org/10.1016/j.jag.2020.102289

Xu P (2009) Iterative generalized cross-validation for fusing heteroscedastic data of inverse ill-posed problems. Geophysical Journal International 179 (1):182-200. doi:10.1111/j.1365-246X.2009.04280.x

Xue F, Lv X, Dou F, Yun Y (2020) A Review of Time-Series Interferometric SAR Techniques: A Tutorial for Surface Deformation Analysis. IEEE Geoscience and Remote Sensing Magazine 8 (1):22-42. doi:10.1109/MGRS.2019.2956165

Yu C, Li Z, Chen J, Hu J-C (2018a) Small Magnitude Co-Seismic Deformation of the 2017 Mw 6.4 Nyingchi Earthquake Revealed by InSAR Measurements with Atmospheric Correction. Remote Sensing 10 (5):684

Yu C, Li Z, Penna NT, Crippa P (2018b) Generic Atmospheric Correction Model for Interferometric Synthetic Aperture Radar Observations. Journal of Geophysical Research: Solid Earth 123 (10):9202-9222. doi:https://doi.org/10.1029/2017JB015305

Yu Y, Li Q, Xu Z, Lü Q, Zhan W, Yao X (2024) An Evaluation of Tropospheric Correction Models for InSAR in Ground Deformation Monitoring: A Case Study in Zhejiang Province, China. Sustainability 16 (11). doi:10.3390/su16114349

Yunjun Z, Fattahi H, Amelung F (2019) Small baseline InSAR time series analysis: Unwrapping error correction and noise reduction. Computers & Geosciences 133:104331. doi:https://doi.org/10.1016/j.cageo.2019.104331

Zhang L, Dong J, Zhang L, Wang Y, Tang W, Liao M (2022) Adaptive Fusion of Multi-Source Tropospheric Delay Estimates for InSAR Deformation Measurements. Frontiers in Environmental Science 10. doi:10.3389/fenvs.2022.859363

Zhou X, Chang N-B, Li S (2009) Applications of SAR Interferometry in Earth and Environmental Science Research. Sensors (Basel, Switzerland) 9 (3):1876-1912. doi:10.3390/s90301876